

# Coupling Reduction of Two Adjacent Quad-Ridge Horn Antennas at 20-40 GHz Using Wideband Electromagnetic Band Gap Structures

Farzad Mohajeri<sup>1\*</sup>, Arman Bordbar<sup>2</sup>, Anis Moradi Kouchi<sup>3</sup>

1- Department of Communication Engineering, Shiraz University, Shiraz, Iran.

Email: mohajeri@shirazu.ac.ir (Corresponding author, Associate professor)

2- Department of Communication Engineering, Shiraz University/ Shiraz, Iran.

Email: armanbordbar1990@gmail.com

3- Department of Communication Engineering, Shiraz University, Shiraz, Iran.

Email: moradi\_a539@yahoo.com

Received: May 2021

Revised: July 2021

Accepted: September 2021

## ABSTRACT:

In this paper, the Electromagnetic Band-Gap (EBG) structures have been used to decrease the mutual coupling between two wideband quad-ridge horn antennas. The EBG structure is a small sheet with a length of 6 cm and a width of 10.6 cm, and it was placed vertically between the horn antennas, providing us with a very compact system. Full-wave CST simulations have been carried out to simulate the whole structure. A two-layer EBG structure has provided a 17 dB isolation over the 20-40 GHz frequency range. Moreover, to verify the proposed structure, EBG layers have been fabricated and measured. The S parameter and far-field measurements of the horn antennas were conducted to investigate the isolation and radiation patterns of the antennas. The measurement results were perfectly comparable with the simulations. Moreover, because of the standalone characteristic of the designed EBGs, this structure can be used as an add-on unit to decrease the E-plane mutual coupling of any two antennas.

**KEYWORDS:** Electromagnetic band-gap, Isolation Parameter, Mushroom, Mutual Coupling, Quad-ridge Horn Antenna, Wideband.

## 1. INTRODUCTION

In some applications, e.g., monostatic radars, commercial repeaters, and phased array antennas, the antennas' separation should be minimized. In contrast, the coupling between antennas sharing common features is a crucial parameter in the design of these systems. Decreasing electromagnetic coupling between the antennas is a challenging task, which has been tackled by many studies. There are some applications, e.g., in-band full-duplex systems, where individual receiving (Rx) and transmitting (Tx) antennas transmit and receive simultaneously on a single channel with the same polarization. A typical value for this application is 110 dB, signal cancellation, requiring the antennas to have more than 60 dB, isolation [1]. In various studies, different approaches have been proposed to increase isolation (decreasing electromagnetic coupling) between two closely-placed antennas. Among the factors that can influence the isolation of two closely-placed antennas, there are separation distance and cross-polarization alignment, which are not usually practical due to some constraints. Two horn antennas that are oriented in the E-

plane show the highest mutual coupling level. Several methods for reducing the E-plane coupling of two rectangular horn antennas are compared through experimental tests. A commonly used method is to isolate the array elements using metal fences [2], [3]. A bed of nails is another method that can produce a high impedance surface (capacitive or inductive) over an octave bandwidth [4], [5]. The monolithic integration of printed electromagnetic band-gap (EBG) structures with microstrip antennas are most commonly utilized by virtue of its compactness and exceptional band-gap characteristics [6-9]. EBG structures are generally defined as periodic (or sometimes non-periodic) structures that block the propagation of electromagnetic waves in a specific frequency band for all radiation angles and polarization states. These structures are usually in a periodic order. They are made of dielectric material and metal conductors. EBG structures have interesting features that make them suitable for a variety of applications. These structures allow the propagation of electromagnetic waves in certain frequency bands and also prevent the propagation of these waves in some

other frequency bands. Another feature that is specific to two-dimensional EBG structures is that the reflection phase due to the collision of plane waves on these surfaces changes in proportion to the frequency. When the plane waves collide the two-dimensional EBG structure, the phase of the structure's reflection coefficient changes with frequency, and at a certain frequency, the phase of the reflection coefficient becomes zero, in which case the EBG structure behaves like a perfect magnetic conductor, which is a phenomenon that it does not exist in nature. When examining the waves within the EBG structure, it is commonly observed that the EBG structure exhibits a frequency stop band in which the frequency range of the waves cannot propagate inside the structure. This feature of preventing the propagation of surface waves is very useful in antenna engineering and has led to the design of antennas with better performance such as higher efficiency. In the field of microwave, this property has been used to control electromagnetic waves and design filters and resonant cavities. Another feature of EBG structures is that they increase the inductance and effective capacitance of the transmission line and prevent the propagation of slow waves. This feature makes the components implemented using EBG structures smaller in size compared to conventional components. There are two general methods for examining the unique properties of EBG structures. The first method is to use full-wave numerical methods. This method describes the properties of EBG structures very accurately but, it is a complex and time-consuming method. Another method that is simpler than the first method is the use of modelling methods of EBG structures, which are often introduced as two modelling methods, the compact element model and the periodic transmission line method. The ease of use of modelling methods reduces their ability to accurately predict all the properties of EBG structures compared to full-wave numerical methods [10].

In this paper, a mushroom-like EBG structure is designed to improve the T/R isolation of two quad-ridge horn antennas operating in K and Ka bands. Measurements demonstrate that isolation between the antennas, separated 13.9 cm edge-to-edge, can be increased from ~60 dB without EBG, to ~78 dB with two EBG sheets. This value increases to ~80 dB for four sheets. The resulting wideband system is simulated using the CST software. In Section 2, CST Microwave Studio is used to simulate the EBG unit cell based on the time-domain solver. Section 3 will be discussed the measured results of the antennas in detail. Also, in this section, magnetic energy density is analyzed. Finally, conclusions are presented in Section 4.

## 2. METHOD

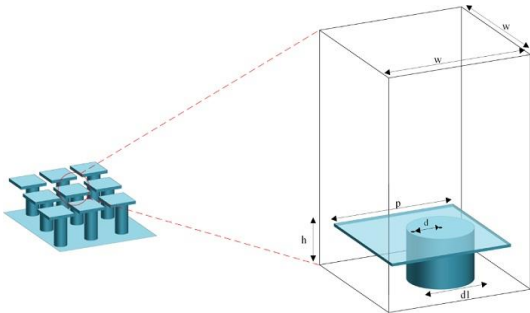
It is proven that a properly designed patch array retains a capacitive reactance over a frequency band broader than that of a bed of nails or a corrugation surface. The bandwidth increment is mostly due to the addition of resonant structure based on the equivalent capacitance and inductance of the patches and vias [4]. The mushroom structure is shown in Fig. 1, and it is considered as a reactive impedance surface. The proposed unit cell structure consists of four components, i.e., a ground plane, a dielectric substrate, metallic patches, and connecting vias [11]. Using a high-impedance metasurface structure that acquires a capacitive reactance over the entire band, it is possible to achieve reasonable isolation in an octave bandwidth. All unit cells' dimensions are designed to increase the bandwidth where the surface reactance ( $X_{TM}$ ) remains capacitive. As the antennas are aligned along the E-plane, the electric field is normal to the surface, and  $X_{TM}$  needs to be capacitive so that RIS can force the electric field to be zero at its surface. The anisotropic surface impedances  $Z_{TM}$  of a homogeneous dielectric, backed by a conductor, can be derived from the reflection coefficients of TM polarized waves ( $\Gamma_{TM}$ ) illuminated on the dielectric surface with an incidence angle of  $\theta$ . It is worth noting that since the structure is far smaller than a wavelength, it can be described by the effective surface impedance [12]. Surface impedances can be calculated using the following equation [13]:

$$Z_{TM} = R_{TM} + jX_{TM} = \frac{\eta_0}{\cos(\theta)} \frac{1 + \Gamma_{TM}}{1 - \Gamma_{TM}} \quad (1)$$

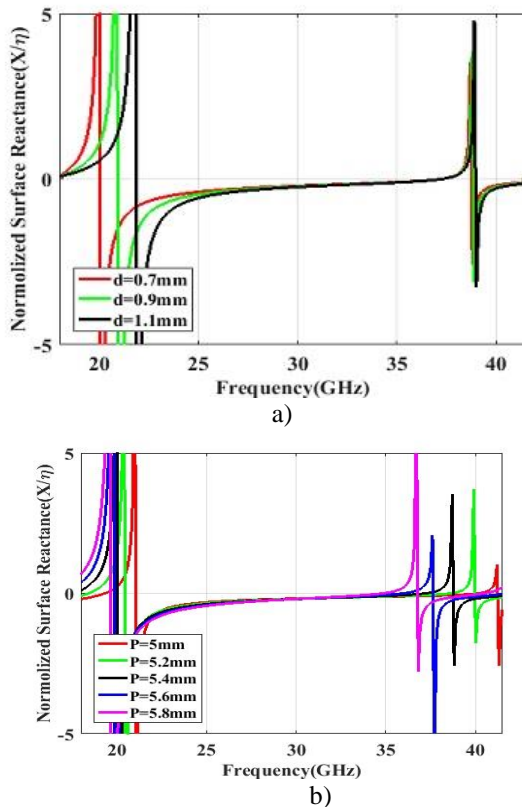
Where,  $R_{TM}$  and  $X_{TM}$  represent the surface resistance and surface reactance, respectively, and  $\eta_0$  is the wave impedance in free space. Based on the analysis, the most significant parameters for designing the metasurface unit cell include patch length ( $p$ ) and the via distance from the patch's center ( $d$ ). In Fig. 2 (a) and (b), the relation of surface impedance with  $p$  and  $d$  is shown.

Fig. 3 depicts the proposed structure setup that is designed for measuring the isolation of antennas in the presence of the EBG metasurface sheets. A low-refractive index material (Teflon) is used to design the stand to ensure that it does not affect the performance of the antenna and the EBG surface. The same pair of horn antennas were used operating at the K and Ka bands and separated by a distance of 13.9 cm. Four EBG surfaces are located (H-plane) between two apertures of the horn antennas. A second setup for measuring the coupling and reflection of the two sheets was repeated. Rogers RO5880 with a dielectric constant of 2.2, a loss tangent of 0.0004, and a height of 1.57 mm is selected as substrate. As was reported in [11], the substrate's thickness is proportional to the inductance in the circuit model, and the inductance in the circuit model has a

direct relationship with the bandwidth. Consequently, in this work, the thickness is set to 1.57 mm, which is relatively thicker than the typical ones. Therefore, a wider bandwidth is achievable, which guarantees the coupling reduction of the antennas. The corresponding finalized dimensions of the mushroom unit cell structure are presented in the legend of Fig. 1.



**Fig. 1.** Perspective view of the designed metasurface unit cell arranged in a square lattice, fabricated as PCB. Physical dimensions are indicated. Substrate material is excluded for clarity ( $d = 0.7$  mm,  $d1 = 0.8$  mm,  $p = 5.4$  mm,  $w = 4.2$  mm, and  $h = 1.54$  mm).



**Fig. 2.** The normalized surface reactance of EBG metasurface for TM polarization as a function of a) position of the via ( $d$ ), b) patch length ( $p$ ).



**Fig. 3.** The setup for measuring the reflection coefficient and coupling of two quad-ridge antennas in the presence of the EBG metasurface.

### 3. RESULTS AND DISCUSSION

#### 3.1. Results

##### 3.1.1. Simulation and Measurement Results

Due to the used setup (Fig. 3) and to investigate whether two or four layers of EBG surfaces are more effective in reducing coupling between antennas, the isolation diagram is plotted for both conditions and the state of without EBG structure. Simulated and measured results are shown in Figs. 4 and 5, respectively. The measurement results show 77 dB isolation between two antennas for the two sheets and 80 dB isolation for the four sheets. This value is 60 dB in the absence of EBG sheets. So, these results show an excellent performance of the proposed structure in improving the isolation between two adjacent antennas. Also, there is a good agreement between simulated and measured results.

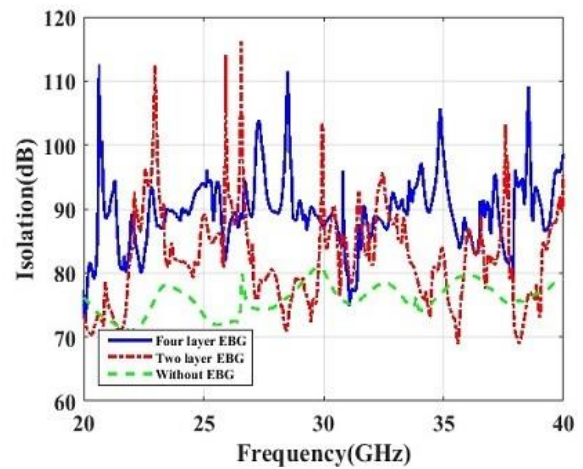


**Fig. 4.** The simulation results for isolation of two quad-ridge horn antennas in three states, two-layer, four-layer EBG, and without an EBG metasurface.

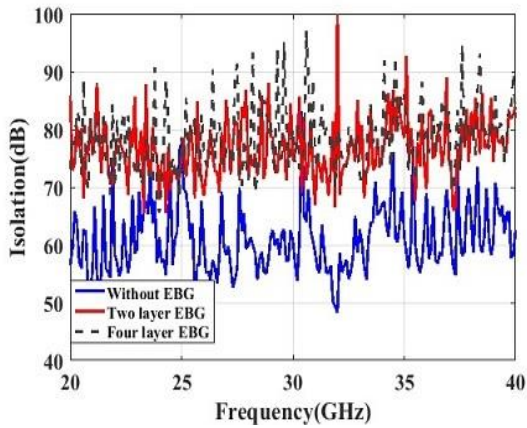
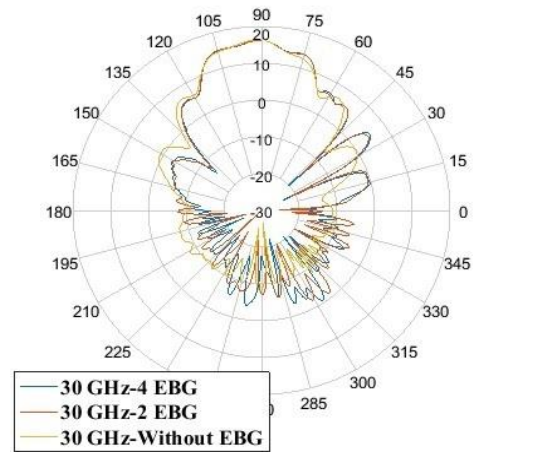


Fig. 5. The measured results for isolation of two quad-ridge horn antennas in three states, two-layer, four-layer EBG, and without an EBG metasurface.

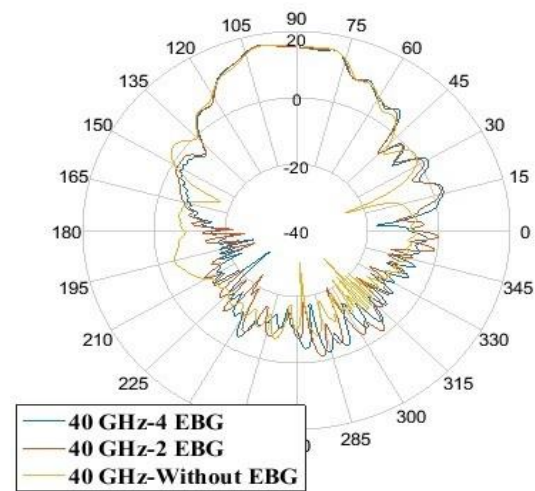
3.1.2. Antenna Radiation Patterns

In this section, the effects of the proposed EBG structure on the radiation pattern of one of the two quad-ridge horn antennas are investigated, experimentally. E-plane cuts of the radiation pattern of the single quad-ridge antenna were measured at 20, 30, and 40 GHz, while one antenna was active and the other one was matched to a 50 Ohm load, in the angular range of 0 to +357° (3° is ignored from the measurements due to physical limitations of measurement setup).

The EBG surface modifies the flow of currents, and the presence of these surfaces will affect the radiation pattern. Simulated and measured radiation patterns are shown in Figs. 6 and 7. As can be seen, the resulting radiation patterns are affected only at higher elevation angles, and the impact on the gain and beamwidth of the antenna is negligible. Also, there is a good agreement between simulated and measured results.

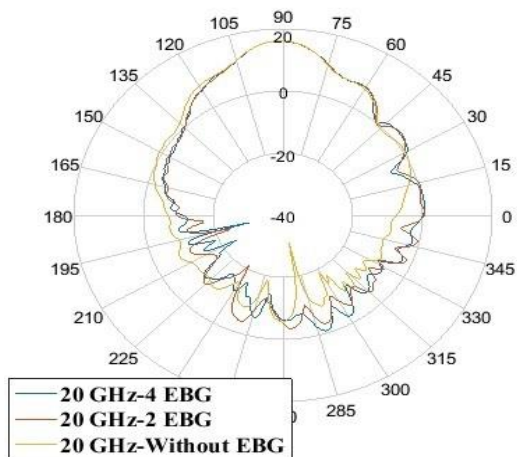


b)

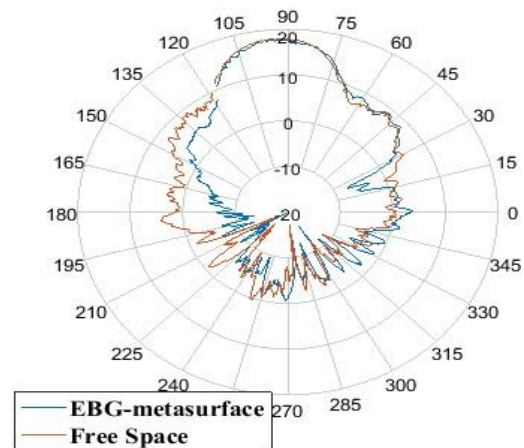


c)

Fig. 6. Simulated radiation patterns for the quad-ridge horn antenna in different cases, i.e., with and without EBG isolator at a) 20 GHz, b) 30 GHz, c) 40 GHz.



a)



a)

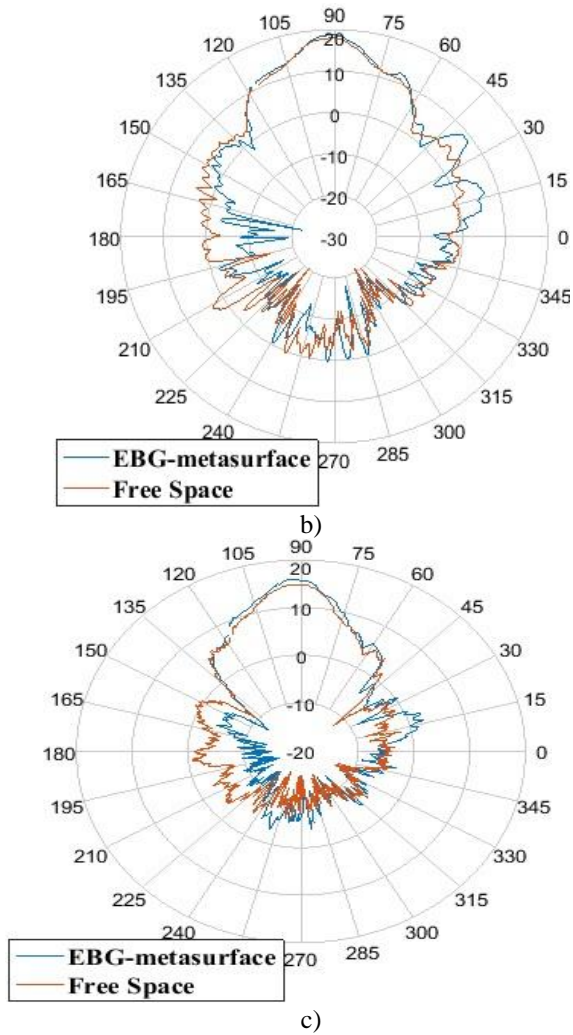


**Fig. 7.** Measured radiation patterns for the quad-ridge horn antenna in different cases, i.e., with 4-EBG and without EBG isolator at a) 20 GHz, b) 30 GHz, c) 40 GHz.

### 3.2. Discussion

The magnetic energy density of the EBG metasurface at 30 GHz is shown in Fig. 8. The magnetic energy density is employed because this EBG surface is composed of a material whose magnetic loss is dominated. The energy density in dB for our setup is indicated in this figure. The active and passive antennas are shown on the left-hand and right-hand sides, respectively. Without the EBG sheet, the magnetic energy density around the passive antenna is about -60 dB (Fig. 8(b)). However, when the EBG sheets separate the antennas, the energy density in the vicinity of the passive antenna falls to -120 dB or lowers (Fig. 8(a)). The coupling is mainly brought about by the spillover or direct radiation through the air from the active antenna.

The horizontal port of the quad-ridge horn antenna is excited, leading to electromagnetic plane waves

propagating along the z-direction. The electric field is along the y-axis (normal to the EBG surface) and the magnetic field along the x-axis. The surface current density on the EBG surface is equal to the tangential component of the magnetic field intensity on it, which is shown in equation (2):

$$\vec{J}_s = \hat{n} \times \vec{H} \quad (2)$$

Where,  $\hat{n}$  is the normal unit vector.

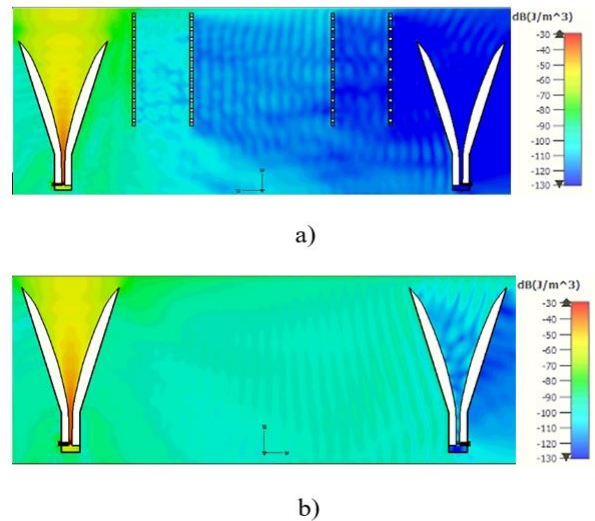


**Fig. 8.** The comparison of magnetic energy density for a pair of horns at 30 GHz a) with EBG metasurface, b) without EBG metasurface.

As shown in Fig. 2, the proposed EBG structure is a high impedance surface, which will deteriorate the tangential component of the magnetic field in the vicinity of EBG sheets and then prevents the flow of surface current on the EBG surface. As a result, this will lead to a high reduction of the coupling between horn antennas and improve their isolation. On the other hand, if a metal sheet has been utilized as an isolator, it does not represent the same performance because the surface current on the metal, led to an increase in the coupling between antennas.

Table 1 compares some of the other techniques for reducing the coupling between antennas with each other and with the proposed method in this paper. It is clearly seen that the proposed EBG structure exhibits much better coupling suppression along with broader bandwidth and standalone capability.

A flowchart, which summarizes the design process to improve isolation and reduce coupling between the two antennas, is shown in Fig. 9.

**Table 1.** Comparison of the proposed decoupling structures and previous works.

Ref.	Center Frequency (GHz)	-10dB Bandwidth (%)	Minimum Coupling Suppression (dB)	Technique	Standalone Capability
[14]	1.09	25	20	Multi-layer EBG structure	Yes
[15]	10	40	15	Dielectric resonator absorber	No
[5]	9	100	10	Bed of nails	No
[16]	10	40	10	EBG surface	No
<b>This work</b>	30	100	20	EBG surface	Yes

**4. CONCLUSION**

An effective isolation structure has been proposed in this study, consisting of two EBG metasurface sheets in the frequency range of K and Ka bands. The EBG unit cell was designed using a time-domain analysis. Based on the full-wave simulations and measurements, it is determined that a decent coupling reduction of 20 dB is

achievable, while the far-field radiation pattern does not have any effects. Since this structure can be used separately, it is applicable for different systems that require high isolation between antennas in a broad frequency band without enlarging the platform.

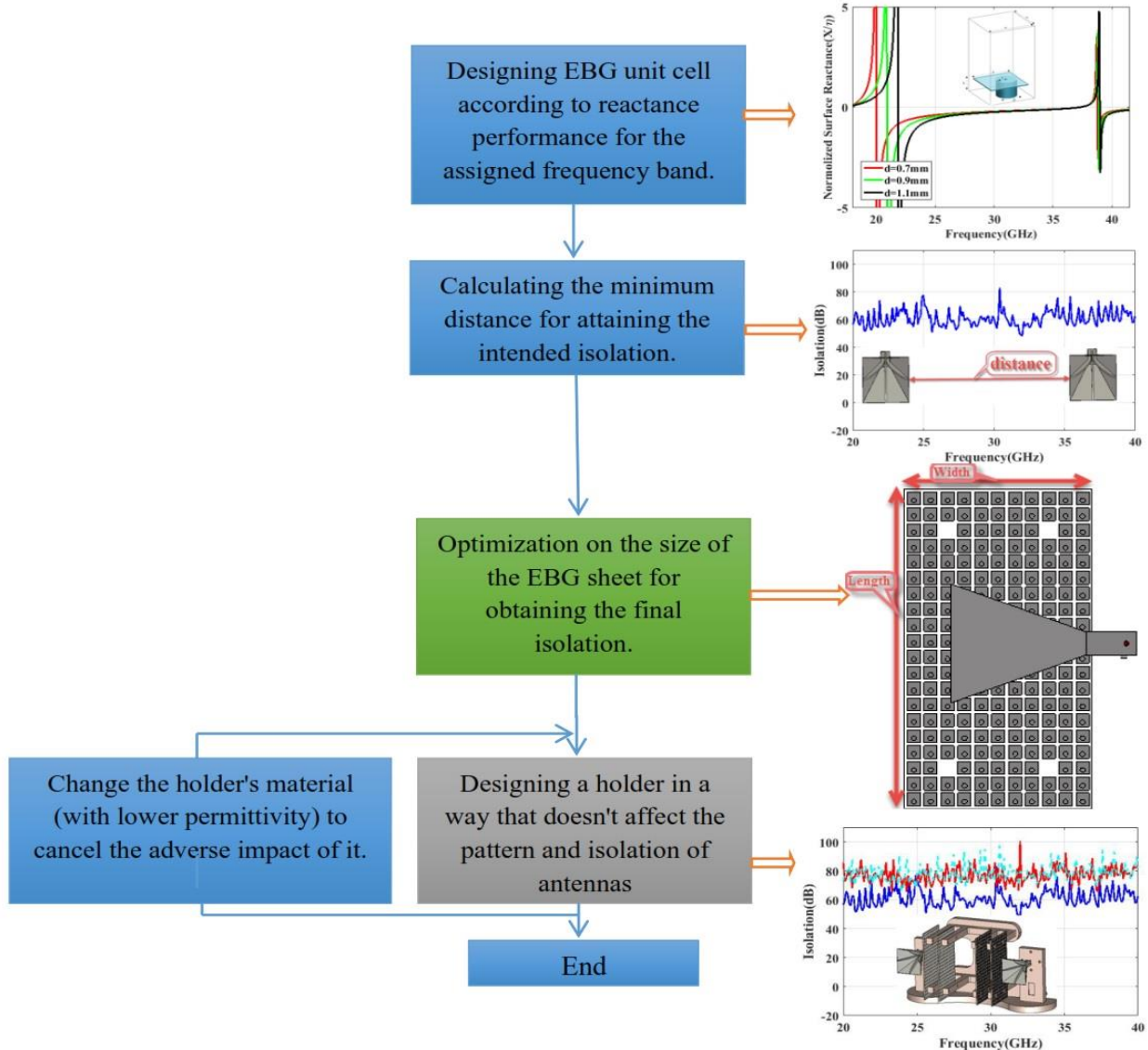


**Fig. 9.** A flowchart of the design process for isolation improvement for any two antennas.

## REFERENCES

- [1] D. Bharadia, E. McMillin, and S. Katti, "Full duplex radios," in *Proceedings of the ACM SIGCOMM 2013 conference on SIGCOMM*, 2013, pp. 375-386.
- [2] J. Lee, "Effects of metal fences on the scan performance of an infinite dipole array," *IEEE Transactions on Antennas and Propagation*, Vol. 38, No. 5, pp. 683-692, 1990.
- [3] M. Van Beurden, A. Smolders, M. Jeuken, G. Van Werkhoven, and E. Kolk, "Analysis of wide-band infinite phased arrays of printed folded dipoles embedded in metallic boxes," *IEEE Transactions on Antennas and Propagation*, Vol. 50, No. 9, pp. 1266-1273, 2002.
- [4] P. V. Prasannakumar, M. A. Elmansouri, and D. S. Filipovic, "Wideband decoupling techniques for dual-polarized bi-static simultaneous transmit and receive antenna subsystem," *IEEE Transactions on Antennas and Propagation*, Vol. 65, No. 10, pp. 4991-5001, 2017.
- [5] P. V. Prasannakumar, M. A. Elmansouri, M. Ignatenko, and D. Filipovic, "Reduction of coupling between flush-mounted antennas," in *2018 International Applied Computational Electromagnetics Society Symposium (ACES)*, 2018, pp. 1-2: IEEE.
- [6] N. Kumar and U. K. Kommuri, "MIMO Antenna H-Plane Isolation Enhancement using UC-EBG Structure and Metal Line Strip for WLAN Applications," *Radioengineering*, Vol. 28, No. 2, pp. 399-406, 2019.
- [7] M. Niroo-Jazi, T. A. Denidni, M. Chaharmir, and A. Sebak, "A hybrid isolator to reduce electromagnetic interactions between Tx/Rx antennas," *IEEE Antennas and Wireless Propagation Letters*, Vol. 13, pp. 75-78, 2013.
- [8] W. Wu, B. Yuan, and A. Wu, "A quad-element UWB-MIMO antenna with band-notch and reduced mutual coupling based on EBG structures," *International journal of Antennas and Propagation*, Vol. 2018, pp. 1-11, 2018.
- [9] X. Yang, Y. Liu, Y. X. Xu, and S.X. Gong, "Isolation enhancement in patch antenna array with fractal UC-EBG structure and cross slot," *IEEE Antennas and Wireless Propagation Letters*, Vol. 16, pp. 2175-2178, 2017.
- [10] F. Yang and Y. Rahmat Samii, "Electromagnetic band gap structures in antenna engineering," *Cambridge University Press*, 2009.
- [11] D. Sievenpiper, L. Zhang, R. F. Broas, N. G. Alexopolous, and E. Yablonovitch, "High-impedance electromagnetic surfaces with a forbidden frequency band," *IEEE Transactions on Microwave Theory and Techniques*, Vol. 47, No. 11, pp. 2059-2074, 1999.
- [12] C. P. Scarborough, Q. Wu, D. H. Werner, E. Lier, R. K. Shaw, and B. G. Martin, "Demonstration of an octave-bandwidth negligible-loss metamaterial horn antenna for satellite applications," *IEEE Transactions on Antennas and Propagation*, Vol. 61, No. 3, pp. 1081-1088, 2012.
- [13] A. Moradi and F. Mohajeri, "Side lobe level reduction and gain enhancement of a pyramidal horn antenna in the presence of metasurfaces," *IET Microwaves, Antennas & Propagation*, Vol. 12, No. 3, pp. 295-301, 2017.
- [14] P. J. Czeresko, A. S. Arman, T. R. Vogler, and M. Ali, "EBG design and analysis for wideband isolation improvement between aircraft blade monopoles," *International Journal of RF and Microwave Computer-Aided Engineering*, Vol. 30, No. 2, p. e22046, 2020.
- [15] S. Hamid and D. Heberling, "Experimental Demonstration of Antenna Isolation Improvement using Planar Resonant Absorbers," in *2019 International Symposium on Electromagnetic Compatibility-EMC EUROPE*, 2019, pp. 351-354: IEEE.
- [16] T. Bertuch, "Comparative investigation of coupling reduction by EBG surfaces for quasi-static RCS measurement systems," *IEEE Antennas and Wireless Propagation Letters*, Vol. 5, p. 231, 2006.